Correlation between superconducting critical temperature and normal-state resistivity parameters from the codoped $ErBa_2Cu_{3-x-y}Zn_xFe_yO_{7-\delta}$ system

Anurag Gupta and Ratan Lal
National Physical Laboratory, K. S. Krishnan Marg, New Delhi 110012, India

A. Sedky
Physics Department, Faculty of Science, Assiut University, Assiut, Egypt

A. V. Narlikar
National Physical Laboratory, K.S. Krishnan Marg, New Delhi 110012, India

V. P. S. Awana
Max-Planck-Institut für Festkörperforschung, Heisenbergstrasse 1, D-70569 Stuttgart, Germany

The Zn and Fe codoped $ErBa_2Cu_{3-x-y}Zn_xFe_yO_{7-\delta}$ system for $0 \leq x \leq 0.45$, $0 \leq y \leq 0.18$, and $0.02 \leq \delta \leq 0.21$ has been investigated. Superconducting critical temperature T_c, residual resistivity ρ_0, resistivity slope corresponding to the linear ρ-T region $(d\rho/dT)_{cc}$, and a characteristic temperature where ρ-T goes through a minima T_{min} are extracted from resistivity measurements. Interestingly, Zn and Fe in general are found to interfere with each other in determining the values of T_c, ρ_0, $(d\rho/dT)_{cc}$, and T_{min}. In one particular case of cosubstitution, T_c is found to enhance. T_c correlates with T_{min}, ρ_0, and $(d\rho/dT)_{cc}$ such that an increase in the former two parameters tends to degrade T_c, while an increase in the latter tends to enhance it. These observations suggest that pinning of the dynamically fluctuating striped phase due to Zn and Fe is a reasonable source of T_c suppression in the present system. We further discuss the reasons and possible consequences of the unusual interference effects of Zn and Fe.

I. INTRODUCTION

Understanding the origin of high-temperature superconductivity by investigating the effect of impurity doping is an approach that has been extensively followed for the last many years.[1] In cuprate superconductors the cationic substitutions attracted such attention almost immediately after the discovery of high-T_c phenomenon in 1986.[2] The fact that during the initial stage the issue relating to the symmetry of the superconducting wave function[3] had received little attention, the role of dopants in providing information about the origin of superconductivity remained obscure. Even today, the results in this respect are although diverse, by and large the current situation seems to be the one that perhaps favors the d-wave pairing.[4] Thus potential scattering, and not magnetic pair breaking, appears to be a possible source of T_c degradation due to incorporation of impurity.[5] In reality the doping effects can be much more complex and intriguing as the impurities may degrade T_c in various other possible ways. One such possibility is the direct suppression of the pairing interaction.[6,7] Another possible origin of T_c degradation is localization,[8] when the localization length becomes comparable to the coherence length. Yet another novel source of suppression of superconductivity caused by pinning of the dynamically fluctuating striped phase has been suggested,[9,10] which is currently gaining considerable theoretical impetus.[11,12]

A proper understanding of the normal state has been considered crucial for an insight into the origin of superconductivity in these systems.[13] And that is where the possible role of an impurity affecting the normal state of the cuprate systems becomes indispensable. In the case of the 1-2-3 system the site-dependent disorder is known to produce different effects.[14] For instance, an impurity disorder at the planar CuO_2 site is found to promote localization of charge carriers, while at the Cu-O chain site it affects the dimensionality and the carrier transport along the c direction. With this background we hope that a study of the 1-2-3 system with simultaneous doping of two kinds of impurities at different sites may provide useful information relevant to the origin of superconductivity. In fact, it may happen that the joint effect of two kinds of impurities on various properties like residual resistivity, resistivity slope, and superconducting critical temperature comes out to be significantly different from that of the direct summation of the effects of the individual impurities.

Specifically, in the present work, we have studied the codoping of Zn and Fe as impurities in the $ErBa_2Cu_3O_{7-\delta}$ (1-2-3) system. The reason for the choice of impurities is that, as it is known for this system,[15–18,2] Zn substitutes at Cu(2) site in the CuO_2 plane, while Fe, at least for low concentrations, substitutes at the Cu(1) site in the Cu-O chain. It would be interesting to examine whether simultaneous presence of these impurities at two different sites of the 1-2-3 structure alters the normal and superconducting state properties, in comparison to their expected individual effects.

II. EXPERIMENTAL DETAILS

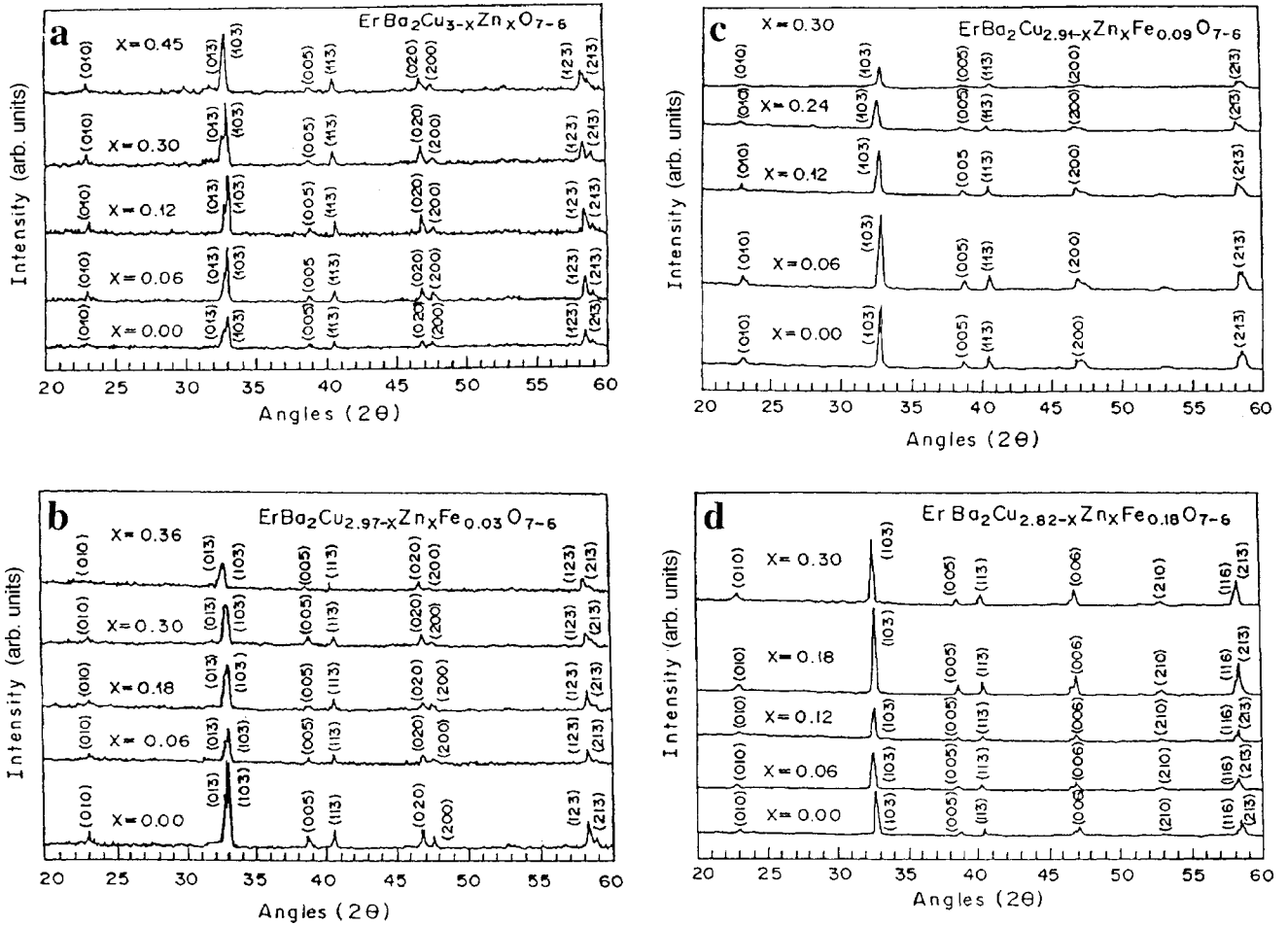Polycrystalline samples of the series $ErBa_2Cu_{3-x-y}Zn_xFe_yO_{7-\delta}$, at different values of x and y

FIG. 1. X-ray diffraction patterns of ErBa$_2$Cu$_{3-x-y}$Zn$_x$Fe$_y$O$_{7-\delta}$ samples with varying Zn content and constant Fe content: (a) $y=0.0$, (b) $y=0.03$, (c) $y=0.09$, and (d) $y=0.18$.

($0 \leq x \leq 0.45$ and $0 \leq y \leq 0.18$) were synthesised through a solid-state reaction method. The ingredients of Er$_2$O$_3$, BaCO$_3$, CuO, ZnO, and FeO$_3$ of $4N$ purity (99.99%) in the stoichiometric ratio 1:2:3 were thoroughly mixed and calcined at 920 °C in air for a period of 16–20 h. After four intermediate grindings and calcination in air the material was crushed, ground, pelletized, and sintered in oxygen for 36 h at 960 °C and then furnace cooled to room temperature with an intervening annealing for 24 h at 600 °C. The samples were characterized for their phase purity by x-ray diffraction (XRD) using a diffractometer equipped with CuKα radiation. The lattice parameters were determined from a least-squares fit of the observed d values. The resistivity was measured in the temperature range of 14–300 K, using four-probe technique in a closed-cycle refrigerator. The oxygen content of the samples was determined by iodometric titration.

III. EXPERIMENTAL RESULTS

A. X-ray diffraction and iodometric titration

In Figs. 1(a)–1(d) we show the x-ray patterns of all the four series of samples of ErBa$_2$Cu$_{3-x-y}$Zn$_x$Fe$_y$O$_{7-\delta}$, for y $=0$, 0.03, 0.09, 0.18, respectively, and for varying Zn content. All the samples were found to be single phase. The calculated a, b, and c lattice parameters, and iodometrically

measured oxygen content for all the samples investigated in the present study are listed in Table I. The observed variation of the lattice parameters and oxygen content as a function of Fe doping for the present series of the sample was very similar to that reported by other workers earlier.[15–18,2] As expected, the oxygen content was found to increase slightly with the increased doping of Fe in the samples. The samples of $y=0.0$ and 0.03 series show an orthorhombic ($a \neq b$) structure, where as those of $y=0.09$ and 0.18 series are all tetragonal ($a=b$). The same can also be appreciated by the observed splitting [Figs. 1(a) and 1(b)] of the (020)-(200) and (123)-(213) reflections showing orthorhombic nature of $y=0.0$ and 0.03 based series, whereas the suppression of the splitting of (020) and (123) reflections [Figs. 1(c) and 1(d)] illustrate the tetragonal nature of $y=0.09$ and 0.18 based series. As a function of Zn content, both the former series of samples with respective constant Fe contents of $y=0.0$ and 0.03 show no change in orthorhombic distortion (OD) for x <0.24, whereafter for $x \geq 0.24$ a decrease in the OD is observed (see Table I). All the four series of samples, with different constant Fe contents, also show a small oxygen loss with increasing Zn content. However, the Cu valence (p^+, see Table I), calculated from the charge neutrality condition for all the samples over the entire studied x and y range, does not show any significant difference compared to the optimum value of 2.28$^+$ observed for the $x=0$, $y=0$ sample.

TABLE I. a, b, and c lattice parameters, orthorhombic distortion [OD$=(b-a)/b$], total oxygen content $(7-\delta)$, effective Cu valence (p^+), and $T_c(\rho=0)$ of a codoped ErBa$_2$Cu$_{3-x-y}$Zn$_x$Fe$_y$O$_{7-\delta}$ system for different values of x and y.

x	y	a (Å)	b (Å)	c (Å)	OD	$7-\delta$	p^+	T_c (K)
0.00	0.00	3.816	3.886	11.683	0.018	6.93	2.28	90.5
0.03	0.00	3.814	3.882	11.684	0.018	6.93	2.29	80.5
0.06	0.00	3.813	3.887	11.683	0.019	6.92	2.29	69
0.12	0.00	3.819	3.881	11.683	0.016	6.92	2.29	52
0.18	0.00	3.818	3.884	11.689	0.017	6.91	2.29	50
0.24	0.00	3.821	3.880	11.690	0.015	6.89	2.28	36
0.30	0.00	3.829	3.876	11.699	0.012	6.86	2.27	32
0.36	0.00	3.834	3.854	11.701	0.005	6.82	2.24	
0.45	0.00	3.838	3.848	11.705	0.003	6.80	2.23	
0.00	0.03	3.836	3.867	11.683	0.008	6.94	2.29	88
0.03	0.03	3.838	3.860	11.682	0.006	6.94	2.29	76
0.06	0.03	3.834	3.865	11.683	0.008	6.93	2.29	63
0.12	0.03	3.839	3.863	11.683	0.006	6.94	2.30	50
0.18	0.03	3.840	3.859	11.686	0.005	6.93	2.30	45.5
0.24	0.03	3.836	3.858	11.688	0.006	6.92	2.30	43
0.30	0.03	3.842	3.856	11.689	0.004	6.88	2.27	
0.36	0.03	3.850	3.855	11.690	0.001	6.85	2.25	
0.00	0.09	3.854	3.854	11.681	0.00	6.96	2.29	83
0.03	0.09	3.859	3.859	11.681	0.00	6.95	2.29	65
0.06	0.09	3.856	3.856	11.680	0.00	6.96	2.29	46
0.12	0.09	3.863	3.863	11.680	0.00	6.95	2.29	41.5
0.18	0.09	3.860	3.860	11.678	0.00	6.94	2.29	36.5
0.24	0.09	3.861	3.861	11.675	0.00	6.94	2.29	31.5
0.30	0.09	3.857	3.857	11.670	0.00	6.90	2.27	
0.00	0.18	3.853	3.853	11.680	0.00	6.97	2.27	71.5
0.03	0.18	3.853	3.853	11.683	0.00	6.97	2.27	44
0.06	0.18	3.856	3.856	11.684	0.00	6.97	2.27	24.5
0.12	0.18	3.856	3.856	11.683	0.00	6.95	2.27	22.5
0.18	0.18	3.851	3.851	11.684	0.00	6.95	2.27	20.5
0.24	0.18	3.854	3.854	11.686	0.00	6.94	2.27	
0.30	0.18	3.851	3.851	11.689	0.00	6.91	2.25	
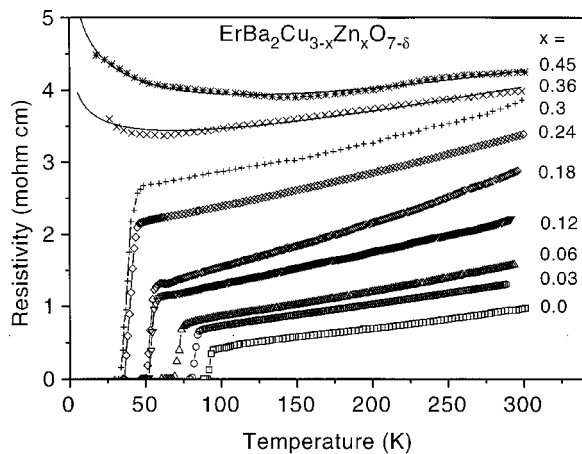
FIG. 2. Resistivity vs temperature for ErBa$_2$Cu$_{3-x-y}$Zn$_x$Fe$_y$O$_{7-\delta}$ samples for different values of Zn content and $y=0.0$. The solid line represents a fit of Eq. (1).

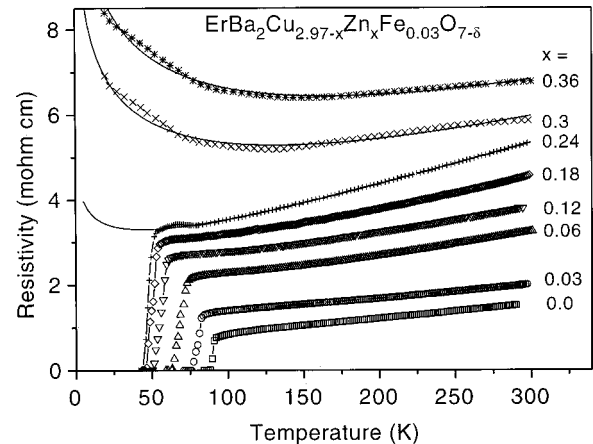FIG. 3. Resistivity vs temperature for ErBa$_2$Cu$_{3-x-y}$Zn$_x$Fe$_y$O$_{7-\delta}$ samples with different values of Zn concentration and $y=0.03$. The solid line represents a fit of the Eq. (1).

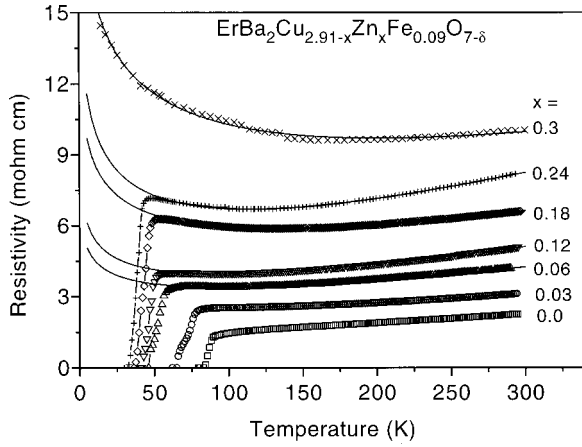FIG. 4. Resistivity vs temperature for $ErBa_2Cu_{3-x-y}Zn_xFe_yO_{7-\delta}$ samples with different values of Zn concentration and $y=0.09$. The solid line represents a fit of the Eq. (1).

B. Normal state resistivity and T_c

Resistivity data as a function of temperature $\rho(T)$ of the $ErBa_2Cu_{3-x-y}Zn_xFe_yO_{7-\delta}$ system for $0 \leq x \leq 0.45$ and $0 \leq y \leq 0.18$ are presented in Figs. 2–5. In general the ρ-T curves involve a linear region, which for low x and y (including $x=y=0$) extends down to a temperature close to $T \approx T_c$, while for higher x and y, the linear region is reduced and persists only until $T > T_c$. The linear part of the ρ-T curves has a positive slope $d\rho/dT$ and its extrapolation to $T=0$ K provides the residual resistivity, say ρ_0. While the ρ_0 is connected with impurity scattering, the slope $d\rho/dT$ determined from the linear region of the ρ-T curve is connected with carrier-carrier scattering. In the following we shall consider only such a resistivity slope and denote it by $(d\rho/dT)_{cc}$, where cc stands for ''carrier-carrier.'' For increasing x and/or y, the ρ-T curves tend to show a minima at a characteristic temperature T_{min}, followed by an upturn ($-ve\ d\rho/dT$) for decreasing temperatures. The upturn may be accounted by a negative $\ln T$ term.[19–21] As shown in Figs. 2–5, in general the ρ-T curves can indeed be fitted well by
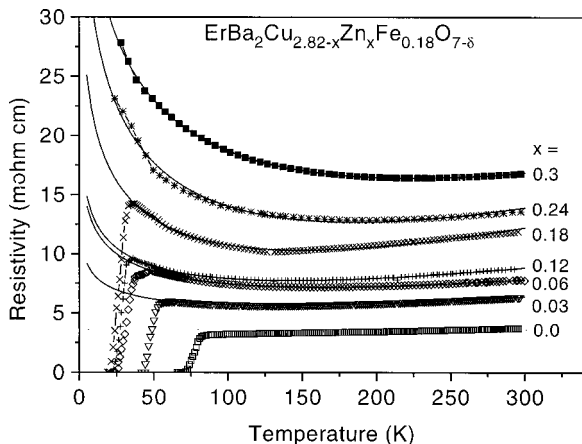
$$\rho = \rho_0 + \rho_1 T - \rho_2 \ln T. \tag{1}$$

FIG. 5. Resistivity vs temperature for $ErBa_2Cu_{3-x-y}Zn_xFe_yO_{7-\delta}$ samples for different values of Zn concentration and $y=0.18$. The solid line represents a fit of the Eq. (1).
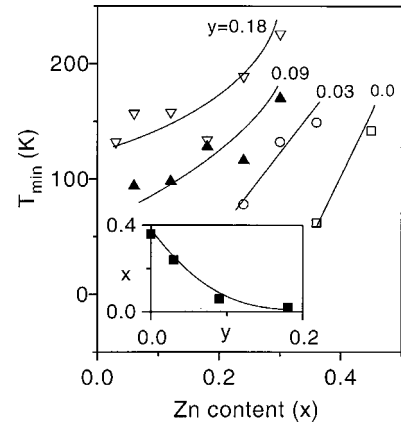

FIG. 6. T_{min} vs Zn content x for different values of Fe content y. Inset: x versus y; x and y correspond to the values where the upturn in $\rho(T)$ is first observed in the 1-2-3 system in Figs. 2–5. The solid lines are a guide to the eye.

The origin of the logarithmic divergence of the resistivity at lower temperatures, in principle, may lie in the Kondo effect,[22] localization,[8] interaction effect,[23] or pinning of the dynamically fluctuating striped phase.[24–26] We shall take up the question of its origin in our samples later in the discussion. Below we first discuss the $\rho(T)$ data to bring out the contrast between individual and combined effects of Zn and Fe doping.

1. Samples containing either Zn or Fe

The $\rho(T)$ data of the Fe-free ($y=0$) Zn-doped samples are shown in Fig. 2. Up to $x=0.12$ (4% Zn) the ρ varies almost linearly with T. In contrast, the $x=0.18$ and 0.30 samples show a nonlinear $\rho(T)$ behavior, which appears to be due to a crossover of one linear region into another linear region of different slope around 175 K and 150 K, respectively.[27] Such a behavior of ρ vs T plots in the Zn-doped system has been reported previously by several authors[28] (see also Ref. 29). The samples with $x \geq 0.36$ show an upturn in $\rho(T)$. The temperature T_{min} where the upturn just begins is found to increase with Zn content. T_{min} as a function of x is shown in Fig. 6. Another feature of the Fe-free Zn-doped samples is that the ρ_0 increases monotonically with the Zn concentration, as depicted in Fig. 7(a). The slope $(d\rho/dT)_{cc}$ increases gradually with increasing Zn concentration until $x=0.3$, whereafter it starts to decrease. This has been shown in Fig. 8. The critical temperatures T_c (estimated from the $\rho=0$ condition) also decrease monotonically with the Zn concentration [cf. Fig. 9(a)]. For up to $x=0.12$ the rate of T_c degradation $|dT_c/dx|$ is about 10 K at. % Zn. This is consistent with earlier observations of other workers on both polycrystalline[15–18,2] and single crystalline material [see Fig. 9(a) for a comparison with results on Zn-substituted single crystals taken from Refs. 28,30]. Thereafter T_c degrades slowly up to $x=0.3$, followed by a rapid suppression again [as seen in Fig. 2, the $\rho(T)$ curves of the samples with $x \geq 0.36$ do not show any sign of superconducting drop down to until 15 K].

The behavior of the $\rho(T)$ for the Zn-free ($x=0$) Fe-doped samples may be seen in the lowest curves of each of the Figs. 2–5. It turns out that ρ varies linearly with T for all
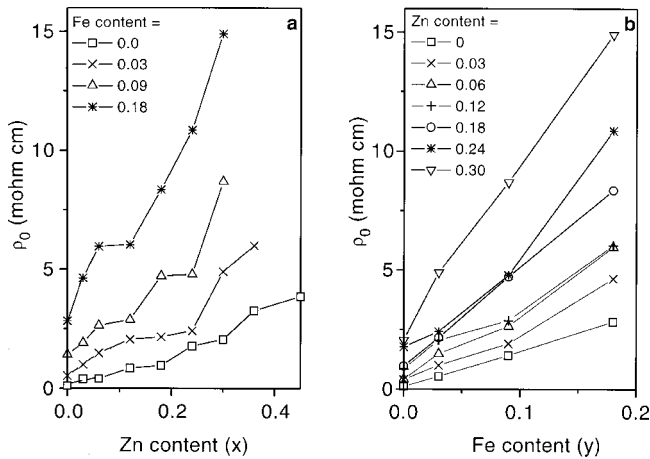
FIG. 7. Residual resistivity ρ_0 vs (a) Zn content x for different values of Fe content y, (b) Fe content y for different values of Zn content x.

the Fe concentration considered here ($y \leq 0.18$). In particular, the T dependence of ρ for the 6% Fe sample ($y = 0.18$, $x = 0$) is qualitatively different from the 6% Zn sample ($x = 0.18$, $y = 0$). Moreover, the residual resistivity ρ_0 is significantly higher in the case of Fe-doped samples of the same concentration as for Zn. For instance, [from Figs. 7(a) and 7(b)], $\rho_0(x = 0.18, y = 0) = 1$ mΩ cm $< \rho_0(x = 0, y = 0.18) = 2.9$ mΩ cm. Despite this, the rate of T_c degradation by Fe [cf. Fig. 9(b)], $|dT_c/dy|$, is much less than that for the corresponding concentration of Zn. In fact, $|dT_c/dy|_{x=0}$ is about 3 K/at. % Fe, which is consistent with the earlier reports on both polycrystalline[15–18,2] and single crystalline material [see Fig. 9(b) for a comparison with results on Fe-
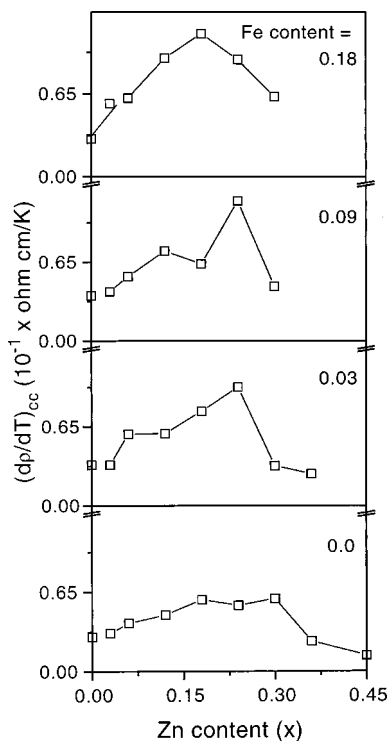

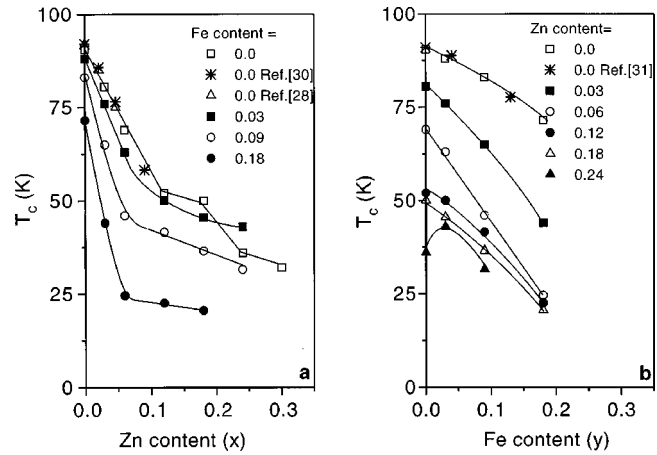FIG. 8. Slope $(d\rho/dT)_{cc}$ vs Zn content x for different values of Fe content y.

FIG. 9. Superconducting transition temperature $T_c(\rho = 0)$ as a function of x and y for ErBa$_2$Cu$_{3-x-y}$Zn$_x$Fe$_y$O$_{7-\delta}$ samples. (a) For varying Zn content and constant Fe content in the samples. Also shown are the data of Zn-doped (Fe-free) 1-2-3 single crystals from Refs. 28,30. Note that the data from Ref. 28 has been shifted up by 3 K for comparison and limited up to $x \leq 0.052$, as crystals in Ref. 28 with higher x show a step in the superconducting transition. (b) For varying Fe content and constant Zn content in the samples. Also shown are the data of Fe-doped (Zn-free) 1-2-3 single crystals from Ref. 31.

substituted single crystals taken from Ref. 31].

While the Fe-free Zn-doped samples and the Zn-free Fe-doped samples show a remarkable difference in their ρ_0 and T_c values, it is surprising to note that for low concentrations in both cases the slope $(d\rho/dT)_{cc}$ seems to be affected by similar magnitudes (Fig. 8). In fact, up to a concentration of 3 at. % of Zn or Fe, $(d\rho/dT)_{cc}$ increases monotonically by about the same magnitudes. For larger concentrations of Zn or Fe, the behavior of $(d\rho/dT)_{cc}$ differs qualitatively as well as quantitatively.

2. Samples containing both Zn and Fe

First we consider the variation of $T_{min}(x,y)$ as shown in Fig. 6 and its inset. The Zn content (x), where an upturn in $\rho(T)$ is first observed in the codoped 1-2-3 samples (see Figs. 2–5), goes down rapidly as a function of increasing Fe content (y) (see inset Fig. 6). From Fig. 6 we find that, for constant Fe content, T_{min} increases rapidly with the further addition of Zn, and vice versa. For instance, the T_{min} of the Fe-free Zn-doped ($x = 0.3$, $y = 0$) sample increases from 60 K to 150 K just by an addition of $y = 0.03$ Fe for the ($x = 0.3$, $y = 0.03$) sample. Whereas, increasing the Zn content by $x = 0.03$ in the Fe-free ($x = 0.3$, $y = 0$) sample would have increased the T_{min} to around 90 K (cf. Fig. 6) only. Similarly, in the case of the Zn-free Fe-doped ($x = 0.0$, $y = 0.18$) sample T_{min} increases from $T < 80$ K to 130 K just by an addition of $x = 0.03$ Zn for the ($x = 0.03$, $y = 0.18$) sample. These are clear signatures of mutual interference of Zn and Fe in determining the normal-state transport behavior of the 1-2-3 system.

The next quantity we consider for the situation of simultaneous presence of Zn and Fe is the residual resistivity $\rho_0(x,y)$. An interesting behavior would be when the combined effect of Zn and Fe, as represented by $\rho_0(x,y)$, is not

a direct summation of the individual effects of Zn and Fe, i.e., when

$$\rho_0(x,y) \neq \rho_0(x,0) + \rho_0(0,y) - \rho_0(0,0). \qquad (2)$$

Here $\rho_0(0,0)$ is subtracted in the right-hand side because the residual resistivity of the pure sample is contained in all $\rho_0(x,y)$, $\rho_0(x,0)$, and $\rho_0(0,y)$. For $\rho_0(x,y)$ to be a direct summation of $\rho_0(x,0)$ and $\rho_0(0,y)$ [to within the residual resistivity of the pure sample, $\rho_0(0,0)$], the $\rho_0(x,y)$ vs x curves, or equivalently the $\rho_0(x,y)$ vs y curves, should be parallel to each other. From Figs. 7(a) and 7(b) we see that this is not the case except for a certain portion of the curves. Thus in general, $\rho_0(x,y)$ is not a direct sum of $\rho_0(x,0)$ and $\rho_0(0,y)$. For example, the $\rho_0(x,0)$ vs x curve is generally superlinear from $x=0.03$ to $x=0.24$. On the other hand, $\rho_0(x,0.03)$ is sublinear for the same range of x. This means that these two curves cannot be connected by a constant change of $\rho_0(0,0.03)$, so that $\rho_0(x,0.03)$ will show a significant interference effect [Eq. (2)].

We now turn to the behavior of $(d\rho/dT)_{cc}$ under the combined effect of Zn and Fe. From Fig. 8 it follows that, for different y, $(d\rho/dT)_{cc}$ as a function of x goes through a maxima, and the corresponding value of x decreases with increasing y. Clearly, for samples with $y=0.0$ ($y=0.18$) the maxima occurs at $x=0.36$ ($x=0.24$). From Fig. 8 we also see that $(d\rho/dT)_{cc}$ vs x curves below the maxima differ qualitatively for different y. For example, for $x=0.03$, the value of $(d\rho/dT)_{cc}$ increases from 0.31 to 0.57 when y increases from 0.0 to 0.18, respectively. In contrast, for the same change in y, the maximum value attained by $(d\rho/dT)_{cc}$ as a function of x increases from 0.60 to 1.12. This means that the combined effect of Zn and Fe for determining $(d\rho/dT)_{cc}$ is not a direct summation of their individually determined $(d\rho/dT)_{cc}$'s.

We next turn to the behavior of T_c under the simultaneous presence of the Zn and Fe atoms. From Fig. 9(a) we see that for low concentrations of Zn ($x \leq 0.06$), addition of Fe impurities increases the rate of suppression of T_c. For $x > 0.06$, because of the presence of Fe, a cross over takes place and the rate of suppression of T_c with Zn is found to be less than that for the Fe-free Zn-doped samples. At higher concentrations of Zn ($x \geq 0.18$), with exact value of x depending upon the Fe content y, T_c gets suppressed rapidly again (refer to the uppermost ρ-T curves, in Figs. 2–5, which do not show any superconducting drop down to 15 K). Another interesting feature of the T_c variation with Zn and Fe is that for the $x=0.24$, $y=0.03$ sample T_c is higher than that for the $x=0.024$, $y=0$ sample [see Fig. 9(a)]. This means that while Zn and Fe both suppress T_c individually, their combined effect may lead to a situation where $T_c(x_1+y_1) > T_c(x_1+y_2)$ with $y_1 > y_2$ [here x_i and y_i ($i=1,2$) are the values of x and y, respectively].

IV. DISCUSSION

A. Correlation of T_c with T_{min}, ρ_0, and $(d\rho/dT)_{cc}$

We now examine the possible correlation of T_c with ρ_0, $(d\rho/dT)_{cc}$, and T_{min} on the basis of their variation extracted above from the data presented in Figs. 2–5.

(1) From Figs. 6 and 9(a), it can be appreciated that in general the higher the T_{min} the lower is the T_c. In other words, it seems that the temperature, at which the logarithmic divergence in $\rho(T)$ occurs, correlates with the T_c of the sample. However, it is interesting to note that such a correlation is strictly true only for the samples compared within any of the four ($y=0.0,0.03,0.09,0.18$) series. It might not work for samples cross compared among different series. For instance, the sample $x=0.03$, $y=0.18$ has a $T_{min}=131$ K and $T_c=44$ K, whereas the sample $x=0.36$, $y=0.0$ has a $T_{min}=62$ K and $T_c < 15$ K.

(2) A comparison of Figs. 7(a) and 9(a) makes it clear that the suppression of T_c with x (for a given y) becomes large or small depending upon whether the corresponding increase of ρ_0 is large or small. This means that T_c correlates with ρ_0. In general, the larger the ρ_0, the smaller is the T_c of the samples. However, as noted above for T_{min}, a strict correlation of T_c and ρ_0 also occurs only for the samples compared within the same series of the samples, and not always for the ones cross compared among different series. For instance, the sample $x=0.03$, $y=0.18$ has a $\rho_0=4.63$ mΩ cm and $T_c=44$ K, where as the sample $x=0.30$, $y=0.0$ has a $\rho_0=2.049$ mΩ cm and $T_c=32$ K. Similarly, comparing the $x=0.24$, $y=0.0$ sample to the $x=0.24$, $y=0.03$ sample, T_c increases despite an increase of ρ_0.

(3) In order to examine how T_c relates with $(d\rho/dT)_{cc}$ we compare Figs. 8 and 9(a). The correlation of T_c with $(d\rho/dT)_{cc}$ is found to be opposite to that shown by ρ_0. For instance, for the values of x, corresponding to the region just below the maxima of $(d\rho/dT)_{cc}$ (see Fig. 8), the rate of decrease of $T_c(x)$ reduces [see Fig. 9(a)] substantially. And for the values of Zn content, corresponding to the region after the maxima of $(d\rho/dT)_{cc}$, the T_c tends to vanish rapidly (refer to the ρ-T curves that do not show superconducting transitions in Figs. 2–5). These results imply that an increase in $(d\rho/dT)_{cc}$ may favor an enhancement in T_c and vice versa. In order to further illustrate that how general this result is, we consider the Zn-doped samples for $0 \leq x \leq 0.24$, and $y=0.0$ and 0.03. The special feature of these samples is that for them ρ_0 changes by a relatively smaller amount for a large range of x. We plot $T_c(y=0.03) - T_c(y=0.0)$ vs $(d\rho/dT)_{cc}|_{y=0.03} - (d\rho/dT)_{cc}|_{y=0.0}$ for different values of x ($0 \leq x \leq 0.24$) in Fig. 10. It is clear that with increased $(d\rho/dT)_{cc}$ the suppression of T_c is reduced, except for the $x=0.06$ and 0.18 samples. Indirectly, this means that in general the increase of $(d\rho/dT)_{cc}$ tends to increase T_c. The increase of T_c of the $x=0.24$, $y=0.03$ sample as compared to the $x=0.24$, $y=0.0$ sample is explained naturally on this basis. In fact, according to Fig. 6 there is a considerable enhancement of $(d\rho/dT)_{cc}$ while going from the $(x,y)=(0.24,0.00)$ sample to the $(x,y)=(0.24,0.03)$ sample. On the other hand, ρ_0 increases relatively only by a smaller amount for the same change in the sample composition [cf. Fig. 7(a)]. Thus it is quite likely that the effect of $(d\rho/dT)_{cc}$ on T_c overpowers the effect of ρ_0, resulting in a net enhancement of T_c.

Further support in favor of this observation comes from the data of the ($x=0.12$, $y=0.09$), ($x=0.12$, $y=0.18$), ($x=0.18$, $y=0.09$), and ($x=0.18$, $y=0.18$) samples. For these samples [cf. Fig. 7(b)] $[\rho_0(y=0.18) - \rho_0(y=0.09)]_{x=0.12}$
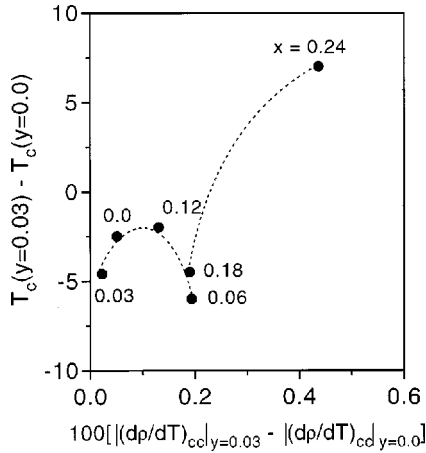
FIG. 10. Relation between $T_c(y=0.03)-T_c(y=0.0)$ vs $|(d\rho/dT)_{cc}|_{y=0.03}-|d\rho/dT)_{cc}|_{y=0.0}$ for samples with varying Zn content.

$\approx[\rho_0(y=0.18)-\rho_0(y=0.09)]_{x=0.18}$. On the other hand, the corresponding difference of $(d\rho/dT)_{cc}$ for $y=0.09$ and $y=0.18$ are much different for $x=0.12$ and $x=0.18$. In fact, $[(d\rho/dT)_{cc}|_{y=0.18}-(d\rho/dT)_{cc}|_{y=0.09}]_{x=0.12}\approx0.15/100$, while $[(d\rho/dT)_{cc}|_{y=0.18}-(d\rho/dT)_{cc}|_{y=0.09}]_{x=0.18}\approx0.50/100$. The decrease of T_c for the case of the $x=0.18$ sample of $y=0.09$ and $y=0.18$ is about 14 K, while it is about 18 K for the $x=0.12$ samples. Since the difference in ρ_0's is almost the same for the two set of samples, and since the difference in $(d\rho/dT)_{cc}$ is more for the $x=0.18$ samples, an increase in $(d\rho/dT)_{cc}$ helps increasing T_c. It may be noted that a similar situation arises also for the $x=0.06$, 0.12 and $y=0.09,0.18$ samples.

B. Possible origin of superconductivity

We have seen that increasing T_{min} and ρ_0 in general tends to degrade T_c, while increasing $(d\rho/dT)_{cc}$ enhances T_c. In cup-rate superconductors this kind of effect of ρ_0 on T_c may arise mainly in two ways. (1) The cuprate superconductors are mainly d-wave superconducting systems.[4] So potential scattering will lead to pair breaking. Since the potential scattering is proportional to ρ_0, increasing ρ_0 implies enhanced pair breaking. Thus T_c will reduce with increasing ρ_0. (2) The other source of reduction of T_c with increasing ρ_0 lies in the pinning of the dynamically fluctuating striped phase. It has been recently[9-12] suggested that pinning of the dynamically fluctuating striped phase may lead to suppression of superconductivity.

In order to see which of these two possibilities, as supported by the present data, determine the connection of T_c with ρ_0 we proceed as follows. We first address the issue of the observed logarithmic divergence of $\rho(T)$ at lower temperatures in both superconducting as well as nonsuperconducting samples (cf. Figs. 2–5). Recently,[24-26] in the underdoped regime, for both La(Sr)-214 and Zn-substituted Y-123 systems, the pinning of a dynamically striped phase has been argued as a possible source of the $-ve\ln T$ behavior of $\rho(T)$. It is interesting to note that although our samples are not in an underdoped regime (see Table I), they still show a logarithmic divergence of $\rho(T)$. We suggest that the observed T_{min} in our doped 1-2-3 samples may mark a change

from a depinned ($T>T_{min}$) to relatively pinned ($T<T_{min}$) striped phase resulting from substitutional disorder due to Zn and Fe.

Now we discuss how such a possibility further determines the connection of T_c with ρ_0. On the basis of the present data we have seen that the suppression of T_c with Zn or Fe is reduced with increasing $(d\rho/dT)_{cc}$. The way we have defined $(d\rho/dT)_{cc}$ makes it clear that its physical origin lies in the carrier-carrier scattering. In fact we do not expect a T-dependent resistivity from carrier-impurity scattering. There may, however, be a T-dependent contribution to the resistivity from electron-phonon scattering. But in cup rates such a contribution is significantly weaker than the contribution due to carrier-carrier scattering. We may, therefore, overlook the electron-phonon scattering rate as compared to the carrier-carrier scattering rate. Increase of $(d\rho/dT)_{cc}$ implies an increase of the carrier-carrier scattering rate unless there is a change in the carrier density and/or density of states at the Fermi level E_F. The Cu valence (p^+, see Table I), over the entire x and y range studied in the present work, does not show any significant variation. We may thus assume that substitution of either Zn and/or Fe does not change the carrier density. This is also supported by earlier studies,[32] where in the case of Zn substitution in the 1-2-3 system, no change was observed in carrier density and density of states at the Fermi level E_F. So, the viewpoint that Zn doping increases the $(d\rho/dT)_{cc}$ implies increase of the carrier-carrier scattering rate.

For Zn-free Fe-doped samples the resistivity ρ varies linearly with temperature for all the Fe concentrations considered here (cf. the lowest ρ-T plots in Figs. 2–5). Thus, there is no signature of (weak) localization in these ($x=0$) samples in the measured temperature range. Moreover, the variation of $(d\rho/dT)_{cc}$ with Fe and Zn concentration is about the same for $x,y\leqslant0.09$. Since Fe substitutes in the Cu-O chains, it seems improbable that it will affect the density of states at E_F, which are mainly determined by the Cu($3d$) and O($2p$) hybridized band of CuO$_2$ planes. On this basis we hope that the increase of $(d\rho/dT)_{cc}$ due to Fe doping also primarily implies increase of the carrier-carrier scattering rate in the samples considered here, although the rate of increment may be quantitatively different from the Zn case.

Thus, in general, the increase of $(d\rho/dT)_{cc}$ appears to imply enhanced carrier-carrier scattering rate $1/\tau_{cc}(T)$ in the samples considered here. But the increase of carrier-carrier scattering rate is known to suppress T_c.[21,33] This contradicts our findings mentioned above. A plausible solution of such a discrepancy is that suppression of T_c due to Zn and/or Fe arises due to pinning of the dynamically fluctuating striped phase. When this is so, ρ_0 will signify the extent of pinning of the striped phase for a given kind of impurity. An impurity tends to pin the dynamically fluctuating striped phase because the impurity is fixed in the lattice. For the case of the carrier-carrier scattering the situation is different because now the source of scattering, a carrier itself, is mobile. Thus, we expect that it (the carrier-carrier scattering) will tend to depin the striped phase. This, in turn, will tend to relatively enhance T_c. In this way, suppression of T_c due to pinning of the striped phase appears to be consistent with the observed correlation of T_c with $(d\rho/dT)_{cc}$ also.

C. Interference effects of the Fe and Zn dopants

We have seen that in general the effect of a simultaneous presence of $(x/3)$ at. % Zn and $(y/3)$ at. % Fe is not equal to the simple addition of the effects of $(x/3)$ at. % Zn (in Fe-free samples) and $(y/3)$ at. % Fe (in Zn-free samples) on the residual resistivity ρ_0, resistivity slope $(d\rho/dT)_{cc}$, T_{min}, and on the transition temperature T_c. We illustrate now that the interference effects of Fe and Zn dopants are expected and follow directly from their different site-dependent impacts on the properties of the 1-2-3 system. Considering that Zn substitutes directly in the CuO_2 plane and Fe occupies the Cu site in the Cu-O chains, the latter can disorder the chains significantly[34] and reduce the coupling of the CuO_2 planes (i.e., more anisotropic) along the c axis.[14] Thus in principle, each of the four series with different constant Fe content ($y=0.0, 0.03, 0.09, 0.18$) should represent series of samples with different anisotropy. In such a case, depending on the value of Fe content in Cu-O chains, Zn doping in CuO_2 planes may result in different functional forms for $\rho_0(x)|_{y=const}$, $(d\rho/dT)_{cc}(x)|_{y=const}$, $T_{min}(x)|_{y=const}$, and $T_c(x)|_{y=const}$. In other words, change in the anisotropy of the 1-2-3 system leads to a change in the electrical transport in the CuO_2 planes, which does not fit with a direct summation of the individual effects of Fe and Zn dopants. The observation of interference effects of Fe and Zn in the 1-2-3 system can explain certain discrepancies and has interesting consequences that we point out below.

An apparent discrepancy that is related to ρ_0, and was not discussed until now, has been that although the rise in ρ_0 is significantly higher in the case of Zn-free Fe-doped samples as compared to the Fe-free Zn-doped samples, the suppression of T_c is much higher in the latter case (see Sec. III B 1). Since the striped phase resides in the CuO_2 planes, and (Zn Fe) substitutes directly in the CuO_2 planes (Cu-O chains), it should pin the striped phase strongly (weakly), leading to a faster (slower) suppression of T_c. Moreover, since Fe doping can cause severe disorder in Cu-O chains, the higher ρ_0 can result partly from the loss of chain conductivity and partly from the increased anisotropy of the 1-2-3 system. The latter cause for increased ρ_0, which probably is linked up with the c-axis transport or the interplanar striped phase interactions, is not completely clear at present.

One interesting occasion where the interference effects of Fe and Zn showed up significantly was the observation of continuous decrease in the Zn content with increasing Fe content in the samples for the evolution of $-ve\ d\rho/dT$ (see inset Fig. 6) in the 1-2-3 system. Since the increase of Fe in Cu-O chains increases the anisotropy of the 1-2-3 system, we infer that higher anisotropy favors the pinning of the dynamically fluctuating striped phase, which is then achieved at smaller Zn content. This can also explain the fact that the increase in T_{min} (Fig. 6) and decrease in T_c [Fig. 9(a)] becomes faster as a function of Zn with the increased codoping of Fe in our samples.

D. Possible extrinsic effects of several factors

The main purpose of the present work was to study the occurrence of superconductivity by probing the Er-1-2-3 polycrystalline system codoped with Fe and Zn. Due to anisotropic nature of the 1-2-3 system, the resistivity of poly-crystalline samples will be mainly determined by the transport along well-connected CuO_2 planes across the grain boundaries. Thus it becomes imperative to ensure that the observed changes in the electrical transport properties of both normal and superconducting states are not caused by any extrinsic microstructure related changes introduced by doping. The possible factors due to doping that can affect the results extrinsically can chiefly be texturing, grain growth/amorphization, and segregation of the dopants at grain boundaries. Before we discuss them, we mention that the chosen ranges of concentration for Zn $(0.0 \leqslant x \leqslant 0.45)$ and Fe $(0.0 \leqslant y \leqslant 0.18)$, for doping the Er-1-2-3 system falls within the solubility regimes reported for Zn [0.0 to 0.3–0.48 (Refs. 16 and 17)] and Fe [0.0 to 0.45– 0.75 (Refs. 15 and 16)]. Although most of the physics discussed in the present work follows from the samples with $x \leqslant 0.30$, the Zn substitution was extended to higher concentrations ($x=0.45$) for the sake of completion. In the XRD patterns [see Figs. 1(a)–1(d)], with increasing x and y, we observe neither an anomalous broadening of any of the peaks, nor an anomalous enhancement of any of the 001 peaks. The former observation suggests no change in grain size, and the latter rules out the possibility of texturing with increased dopant addition. The third factor of grain boundary segregation of dopants is also quite improbable, as that should amount to nonstochiometry in the samples and result in proportionately increasing unreacted dopants and CuO, which are not seen to within 3% in the XRD patterns. Also, a good agreement of $T_c(x)$ and $T_c(y)$ observed [cf. Figs. 9(a) and 9(b)] between our polycrystalline samples and single crystals negates the possibility of grain boundary segregation of dopants.

Next, any inhomogeneity at the grain boundaries should also result in a T_c distribution that could have manifested itself in the $\rho(T)$ behavior near the onset and when ρ goes to zero. Out of a total of 31 samples used in this work, two samples $x=0.03$, $y=0.09$ and $x=0.06$, $y=0.18$ show a slight broadening near the onset (see Figs. 3 and 4), which even if removed do not affect the present analysis. Besides them, none of the 29 samples, as depicted in Figs. 2–5, show any broadening near superconducting onset and/or a tail at temperatures where ρ goes to zero. Actually some of the transitions get sharper at higher dopant concentrations. For instance, from Fig. 2, the sample with $x=0.06$, $y=0.0$ has a $\Delta T_c \approx 6$ K, whereas the sample with higher Zn content $x=0.18$, $y=0.0$ has a $\Delta T_c \approx 4$ K. Similarly, as seen in Fig. 3, the samples with $x=0.06$, $y=0.03$ and $x=0.24$, $y=0.03$ show $\Delta T_c s = 10$ K and 5 K, respectively. We would also like to remark that after a certain concentration if any of the dopants Fe and Zn or a combination of both starts to segregate at the grain boundaries, it should result in a signature of incomplete superconducting transition (coming from the doped intragranular material) in the $\rho(T)$ graphs, which is not observed (see the topmost graphs in Figs. 2–5).

Considering these observations and the fact that all our samples are prepared under identical synthesis conditions, we feel, the present analysis of doping with respect to a pure sample is justified as a first approximation. Finally, in high-temperature superconductors (HTSCs) doped with impurities, we believe that the microstructure may not be strongly correlated with the suppression of superconductivity. Important evidence of this is the observation of similar rates of T_c

depression with increased dopant concentration, in both single crystals and polycrystalline materials, e.g., in the case of the 1-2-3 system doped only with Zn or Fe, see Fig. 9. Second, there are models (Phillips[35]) that explain the behavior of HTSCs on the basis of quantum percolation, which need disorder at nanoscale, and make the microstructural details redundant as far as the mechanism of superconductivity is concerned.

V. CONCLUSIONS

In this paper we have presented results of resistivity vs temperature behavior for the codoped $ErBa_2Cu_{3-x-y}Zn_xFe_yO_{7-\delta}$ system. From the ρ-T curves we have extracted the residual resistivity $\rho_0(x,y)$, resistivity slope corresponding to the carrier-carrier scattering $(d\rho/dT)_{cc}$, a characteristic temperature marking the upturn in ρ-T curves T_{min}, and the critical temperature T_c. On the basis of these parameters it is found that in general the impurities Zn and Fe interfere with each other significantly. The plausible reason for this has been identified with different site-dependent impacts of Zn (in CuO_2 planes) and Fe (in Cu-O chains), where the latter effects the anisotropy of the 1-2-3 system. As a consequence of this ρ_0, $(d\rho/dT)_{cc}$, T_{min}, or T_c cannot be expressed, in general, as a direct sum of the individual effects of Zn and Fe.

An attempt has been made to understand the correlation of T_c with T_{min}, ρ_0, and $(d\rho/dT)_{cc}$. It is found that increasing T_{min} and ρ_0 tends to suppress T_c, while increasing $(d\rho/dT)_{cc}$ tends to enhance T_c. On the basis of the generally acclaimed belief that the cup-rate superconductors are d-wave superconductors, it has been argued that potential scattering is not adequate for explaining the correlation of T_c with T_{min}, ρ_0, and $(d\rho/dT)_{cc}$ simultaneously. We proposed that T_{min}, which marks the onset of logarithmic divergence of $\rho(T)$ observed at low temperatures, may characterize a crossover temperature from a depinned to a relatively pinned striped phase. Further, pinning of the dynamically fluctuating striped phase in accordance with T_{min} and ρ_0 and depinning of this phase due to $(d\rho/dT)_{cc}$ gives a plausible explanation for the observed correlation of T_c with T_{min}, ρ_0, and $(d\rho/dT)_{cc}$.

[1] D. Belitz, Phys. Rev. B **35**, 1636 (1987); **35**, 1651 (1987); **36**, 47 (1987).

[2] A. V. Narlikar, C. V. N. Rao, and S. K. Agarwal, in *Studies of High Temperature Superconductors*, edited by A. V. Narlikar (Nova Science, New York, 1989), Vol. 1, p. 341.

[3] R. Combescot and X. Leyronas, Phys. Rev. Lett. **75**, 3732 (1995).

[4] R. B. Laughlin, Phys. Rev. Lett. **80**, 5188 (1998).

[5] A. J. Millis, S. Sachdev, and C. M. Varma, Phys. Rev. B **37**, 4975 (1988).

[6] Ratan Lal, Phys. Rev. B **51**, 640 (1995).

[7] G. V. M. Williams, J. L. Tallon, and R. Meinhold, Phys. Rev. B **52**, 7034 (1995).

[8] M. V. Sadovskii, in *Studies of High Temperature Superconductors* (Ref. 2), Vol. 11, p. 131.

[9] G. D. Liu, Z. X. Zhao, and G. C. Che, Solid State Commun. **109**, 495 (1999).

[10] J. S. Zhou, J. B. Goodenough, H. Sato and M. Naito, Phys. Rev. B **59**, 3827 (1999).

[11] R. F. Service, Science **283**, 1106 (1999).

[12] N. Hasselmann, A. H. Castro Neto, C. Morair Smith, and Y. Dimashko, Phys. Rev. Lett. **82**, 2135 (1999).

[13] P. W. Anderson, *The Theory of Superconductivity in the High-T_c Cuprates* (Princeton University, Princeton, 1997).

[14] A. K. Bandyopadhyay, D. Varandani, E. Gmelin, and A. V. Narlikar, Phys. Rev. B **50**, 462 (1994).

[15] M. Mehbod, P. Wyder, R. Deltour, Ph. Duvigneaud, and G. Maessens, Phys. Rev. B **36**, 8819 (1987).

[16] J. M. Tarascon, P. Barboux, P. F. Miceli, L. H. Greene, G. W. Hull, M. Eibschutz, and S. A. Sunshine, Phys. Rev. B **37**, 7458 (1988).

[17] G. Xiao, M. Z. Cieplak, A. Gavrin, F. H. Streitz, A. Bakhshai, and C. L. Chien, Phys. Rev. Lett. **60**, 1446 (1988).

[18] Y. Xu, R. L. Sabatini, A. R. Moodenbaugh, Y. Zhu, S. G. Shyu, M. Suenaga, K. W. Dennis, and R. W. McCallum, Physica C **169**, 205 (1990).

[19] V. Kataev, V. Kataev, Yu. Greznev, G. Teitel'baum, M. Breuer, and N. Knauf, Phys. Rev. B **48**, 13 042 (1993).

[20] Rajvir Singh, R. Lal, U. C. Upreti, D. K. Suri, A. V. Narlikar, V. P. S. Awana, J. Albino Aguiar, and Md. Shahabuddin, Phys. Rev. B **55**, 1216 (1997).

[21] Very recently Musa *et al.* [J. E. Musa, S. Garcia, M. Rothier de Amaral, Jr., H. Salim de Amorim, B. Giordanengo, E. M. Baggio-Staitovitch, P. J. G. Pagliuro, C. Rettori, W. B. Yelon, and S. K. Malik, Phys. Rev. B **59**, 6557 (1999)] have measured the resistivity of the $(La_{1-x}Pr_x)_{1.85}Sr_{0.15}CuO_4$ system for different values of Pr concentration x. They have fitted their data with Eq. (1) of this paper. They have found that T_c of the $(La_{1-x}Pr_x)_{1.85}Sr_{0.15}CuO_4$ system correlates well with ρ_2. This observation of Musa *et al.* is incomplete in that the T_c of the samples considered by them also correlates well with the resistivity slope $(d\rho/dT)_{cc}$, such that increasing $(d\rho/dT)_{cc}$ enhances T_c suppression.

[22] J. Kondo, in *Solid State Physics: Advances in Research and Applications*, edited by H. Ehrenreich, F. Seitz, and D. Turnbull (Academic, New York, 1969), Vol. 23, p. 183.

[23] B. L. Altshuler and A. G. Aronov, Solid State Commun. **39**, 115 (1979).

[24] Y. Ando, G. S. Boebinger, A. Passner, T. Kimura, and K. Kishio, Phys. Rev. Lett. **75**, 4662 (1995).

[25] J. M. Tranquada, J. D. Axe, N. Ichikawa, Y. Nakmura, S. Uchida, and B. Nachumi, Phys. Rev. B **54**, 7489 (1996).

[26] Kouji Segawa and Yoichi Ando, Phys. Rev. B **59**, R3948 (1999).

[27] A possible reason for such a behavior may be activation of certain phonon modes for certain dopant concentration above a suitable temperature. Such modes may couple with electrons to increase the electron-electron scattering rate in an effective way.

[28] Chien *et al.* [T. R. Chien, Z. Z. Wang, and N. P. Ong, Phys. Rev. Lett. **67**, 2088 (1991)] have found that the single crystal of $YBa_2Cu_3O_{7-\delta}$ doped with 0.53% Zn shows a superlinear ρ-T behavior, similar to that observed for the $ErBa_2Cu_3O_{7-\delta}$ sample of 6.0% Zn in the present case. The temperature where the superlinear behavior of ρ-T appears to be a crossover of two linear behaviors is $T^* \approx 160$ K for the 0.53% Zn samples of $YBa_2Cu_3O_{7-\delta}$, as compared to $T^* \approx 175$ K in the present case. There are other cases also where the ρ-T curve shows a superlinear behavior. The 2%, 8/3% and 10/3% Zn-doped samples of polycrystalline $DyBa_2Cu_3O_{7-\delta}$ also show superlinear behavior near $T^* \approx 170$ K [S. S. Ata-Allah, Y. Xu, and Ch. Heiden, Physica C **221**, 39 (1994)]. A superlinear behavior of the ρ vs T curve is also seen in the 3% Zn sample of polycrystalline $YBa_2Cu_3O_{6.95}$ and with $T^* \approx 180$ K [D. J. C. Walker, A. P. Mackenzie, and J. R. Cooper, Phys. Rev. B **51**, 15 653 (1995)].

[29] For the samples where ρ-T behavior may be approximated as a crossover from one linear region with lower slope to another with higher slope, we have defined $(d\rho/dT)_{cc}$ by the linear region nearer to T_c. A similar specification for $d\rho/dT$ has been considered earlier [D. J. C. Walker, A. P. Mackenzie, and J. R. Cooper, Phys. Rev. B **51**, 15 653 (1995)].

[30] Kouichi Semba, Azusa Matsuda, and Takao Ishii, Phys. Rev. B **49**, 10 043 (1994).

[31] M. D. Lan, J. Z. Liu, Y. X. Jia, Y. Nagata, P. Klavins, and R. N. Shelton, Phys. Rev. B **47**, 457 (1993).

[32] See, for example, Ref. 7.

[33] As we have already clarified $(d\rho/dT)_{cc}$ corresponds to carrier-carrier scattering. But carrier-carrier scattering amounts to reducing the mean free path of the carrier. Such a situation tends to reduce T_c by breaking Cooper pairs near T_c (cf. Ref. 5).

[34] G. G. Li, F. Bridges, J. B. Boyce, and W. C. H. Jainer, Phys. Rev. B **47**, 12 110 (1993).

[35] J. C. Phillips, Proc. Natl. Acad. Sci. USA **94**, 12 774 (1997).